

Imaging of in vitro and in vivo bones and joints with continuous-wave diffuse optical tomography

Yong Xu, Nicusor Iftimia, and Huabei Jiang

*Department of Physics & Astronomy, Clemson University, Clemson, SC 29634
hjiang@clemson.edu*

L. Lyndon Key

*Department of Pediatrics and General Clinical Research Center,
Medical University of South Carolina, Charleston, SC 29425*

Marcy B. Bolster

*Division of Rheumatology and Immunology, Medical University of South Carolina,
Charleston, SC 29425*

<http://virtual.clemson.edu/groups/bmol>

Abstract: We present what is believed to be the first absorption and scattering images of in vitro and in vivo bones and joints from continuous-wave tomographic measurements. Human finger and chicken bones embedded in cylindrical scattering media were imaged at multiple transverse planes with Clemson multi-channel diffuse optical imager. Both absorption and scattering images were obtained using our nonlinear, finite element based reconstruction algorithm. This study shows that diffuse optical tomography (DOT) has the potential to be used for detection and monitoring of bone and joint diseases such as osteoporosis and arthritis.

© 2001 Optical Society of America

OCIS codes: (110.6960) Tomography; (170.3010) Image reconstruction techniques; (170.3660) Light propagation in tissues

References and links

1. S. Colak, M. van der Mark, G. tHooft, J. Hoogenraad, E. van der Linden, F. Kuijpers, "Clinical optical tomography and NIR spectroscopy for breast cancer detection," *IEEE J. Sel. Top. Quant. Electron.* **5**, 1143-1158(1999).
2. V. Ntziachristos, A. Yodh, M. Schnall, B. Chance, "Concurrent MRI and diffuse optical tomography of breast after indocyanine green enhancement," *Proc. Natl. Acad. Sci. USA* **97**, 2767-2772(2000).
3. H. Jiang, N. Iftimia, J. Eggert, L. Baron, K. Klove, Y. Xu, Y. Yang, T. Pope, "Near-infrared optical imaging of breast," *Med. Phys.* (in press).
4. B. Chance, E. Anday, S. Nioka, S. Zhou, L. Hong, K. Worden, C. Li, T. Murray, Y. Ovetsky, D. Pidikiti, R. Thomas, "A novel method for fast imaging of brain function, non-invasively, with light," *Opt. Express* **2**, 411-423(1998), <http://www.opticsexpress.org/oearchive/source/4445.htm>
5. V. Prapavat, R. Schuetz, W. Runge, J. Beuthan, G. Muller, "In vivo investigations on the detection of chronic polyarthritis using a cw transillumination method at interphalangeal joints," *Proc. SPIE* **2626**, 360-366(1995).
6. B. Devaraj, M. Takeda, M. Kobayashi, M. Usa, K. Chan, Y. Watanabe, T. Yuasa, T. Akatsuka, M. Yamada, H. Inaba, "In vivo laser computed tomographic imaging of human fingers by coherent detection imaging method using different wavelengths in near infrared region," *Appl. Phys. Lett.* **69**, 3671-3673(1996).
7. M. Zevallos, S. Gayen, B. Das, M. Alrubaiee, R. Alfano, "Picosecond electronic time-gated imaging of bones in tissues," *IEEE J. Sel. Top. Quant. Electron.* **5**, 916-922(1999).
8. A. Klose, A. Hielscher, K. Hanson, J. Beuthan, "Two- and three-dimensional optical tomography of finger joints for diagnostics of rheumatoid arthritis," *Proc. SPIE* **3566**, 151-159(1998).

9. N. Iftimia, H. Jiang, "Quantitative optical image reconstruction of turbid media using dc measurements," *Appl. Opt.* **39**, 5256-5261(2000).
 10. J. Beuthan, O. Minet, G. Muller, V. Prapavat, "IR-diaphanoscopy in medicine," in *Medical Optical Tomography: Functional Imaging and Monitoring* (G. Muller, B. Chance, R. Alfano, eds.), pp. 263-282, SPIE Press, 1993.
 11. V. Prapavat, W. Runge, J. Mans, A. Krause, J. Beuthan, G. Muller, "The development of a finger joint phantom for the optical simulation of early inflammatory rheumatic changes," *Biomedizinische Technik* **42**, 319-326(1997).
 12. J. Beuthan, V. Prapavat, R. Naber, O. Minet, G. Muller, "Diagnostic of inflammatory rheumatic diseases with photon density waves," *Proc. SPIE* **2676**, 43-53(1996).
-

1. Introduction

Near-infrared diffuse optical tomography (DOT) has found its applications in imaging thick tissues such as breast and brain due to its unique capability of extracting tissue functional information.¹⁻⁴ Analogously, DOT could be used for imaging other tissues such as human joints and associated bones. Diseases related to bones and joints such as osteoporosis and arthritis are major cause of morbidity in the population over 50, affecting more than 68 million Americans. Conventional imaging modalities including x-ray radiography, computed tomography (CT), magnetic resonance imaging (MRI) and ultrasonography usually can provide only tissue structural information which limits their use especially for early detection of diseases.

Direct optical methods have been successfully used to image human finger joints and bones with time-independent, continuous-wave (cw) and time-resolved measurements.⁵⁻⁷ Since these direct optical imaging techniques use measured optical data themselves to form images, they can provide only structural information of tissues, and may not be able to take full advantage of all the information contained in the data collected. The idea of DOT is to extract the spatial maps of intrinsic tissue absorption and scattering coefficients from the measured optical data through model-based reconstruction methods; thus tissue functional information and higher image resolution can be obtained with DOT. DOT has been recently proposed for imaging joint tissues, but limited to only numerical simulations, to the best of our knowledge.⁸ In this paper, we report for the first time both absorption and scattering images of in vitro and in vivo bones and joints using cw tomographic measurements.

2. Materials and Methods

Our DOT imager is an automated multi-channel frequency-domain system, shown in Fig. 1 (we just needed dc measurements to reconstruct the absorption and scattering images reported here). In this system, an intensity-modulated light from a 785-nm 50 mW diode laser is sequentially sent to the sample by 16 3-mm fiber optic bundles. For each source position, the diffused light is received at 16 detector positions along the surface of the sample and sequentially delivered to a photomultiplier tube (PMT). A second PMT is used to record the reference signal. The multiplexing of the source/detector fibers is accomplished by two automatic moving stages. dc, ac and phase shift signals are obtained using the standard heterodyne technique controlled by Fast Fourier Transform (FFT) Labview routines. The measured dc data are then input into our reconstruction software to generate a 2D cross-sectional image of the medium/tissue at the source-detector plane. Both source and detector fiber bundles are firmly held by a metal ring structure with a diameter of 5 cm. 16 detector fiber bundles are arranged equally-spaced around the annulus with another 16 source fiber bundles interspersed between the detector bundles. In the current configuration individual source and detector fibers are mechanically translated past single illumination and detection subsystems. At present, data collection time is about 10 minutes per measurement plane.

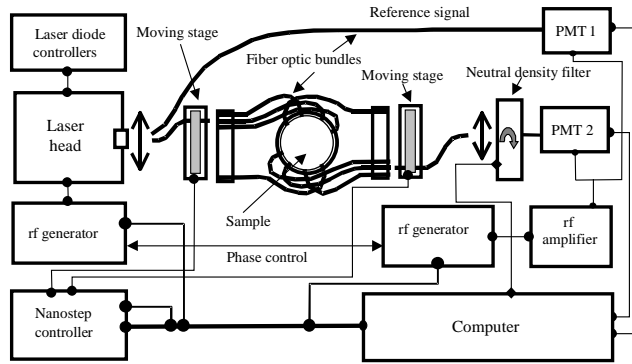


Fig. 1: Schematic of the DOT system.

For the *in vitro* experiment, the sample consisted of two chicken bones embedded in a cylindrical solid phantom with a diameter of 5 cm. The solid phantom has contained a scattering medium composed of Intralipid (a fat emulsion suspension) with India ink as an absorber, which has had $\mu_a = 0.005 \text{ mm}^{-1}$ (absorption coefficient) and $\mu'_s = 1.0 \text{ mm}^{-1}$ (reduced scattering coefficient). Agar powders have been used to solidify the Intralipid/ink suspensions. A schematic of this phantom is given in Fig. 2a where it also shows that the tomographic measurements have been conducted at two different planes. For the *in vivo* experiment, the sample was the index finger of a male volunteer inserted into the same cylindrical solid phantom. Fig. 2b displays a schematic of the finger measurement configuration. A translation stage coupled with a high precision digital scale was used to vertically position the ring holding the source and detector fibers. The *in vivo* tomographic measurements have been conducted at the joint and off-joint/bone different planes, as shown in Fig. 2b. Both absorption and scattering images of the sample were recovered using our nonlinear, finite element based reconstruction algorithm, which was described in detail elsewhere.⁹ This algorithm uses a regularized Newton's method to update an initial optical property distribution iteratively in order to minimize an object function composed of a weighted sum of the squared difference between computed and measured optical data at the sample surface. The 2D finite-element mesh used had 257 nodes and 448 elements for both forward and inverse solutions. The images reported here were results of 30 iterations. The computations were performed in a 700 MHz Pentium III PC.

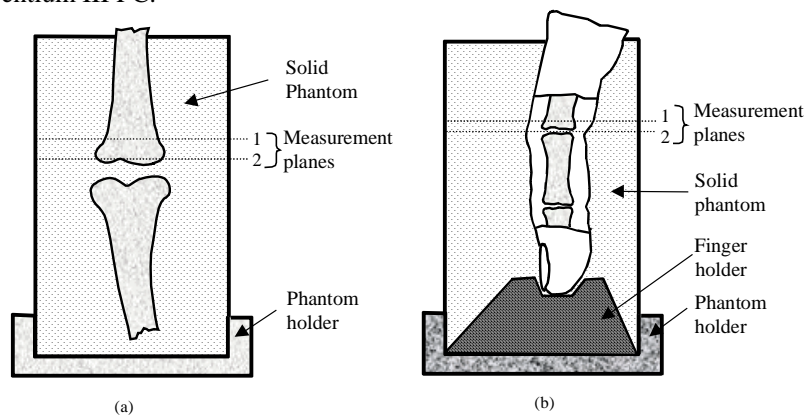


Fig. 2: (a) schematic of our test configuration including the solid phantom, chicken bones, and measurement planes. (b) schematic of the finger measurement configuration.

3. Results and Discussion

Fig. 3 presents the absorption and scattering images at two measurement planes from the phantom measurements. As can be seen, both absorption and scattering images exhibit a marked absorption or scattering increase at the bone region compared to the phantom background. The bone size can be measured based on the full width at half maximum of the recovered bone optical properties. Using this threshold, we note that the bone size resolved by DOT is 1.50 cm, which is comparable to the actual bone size (≈ 1.60 cm). The average bone absorption and reduced scattering coefficients are found to be 0.021/mm and 1.75/mm respectively.

Fig. 4 displays the optical images at the joint and off-joint planes from the in vivo measurements. We note that both absorption and scattering images show a significant absorption or scattering increase in the joint and off-joint bone regions related to the surrounding soft tissue and phantom background. The bone size optically imaged is 1.65 cm which is also comparable to the actual size of bone in the finger (≈ 1.70 cm). The average bone absorption and reduced scattering coefficients are calculated to be 0.023/mm and 2.14/mm, respectively. The joint dominated by synovial membrane and fluid has significantly smaller absorption and scattering coefficients than the bone region, and they are found to be 0.011/mm and 1.81/mm, respectively. These values are consistent with those reported in the literature.¹⁰⁻¹²

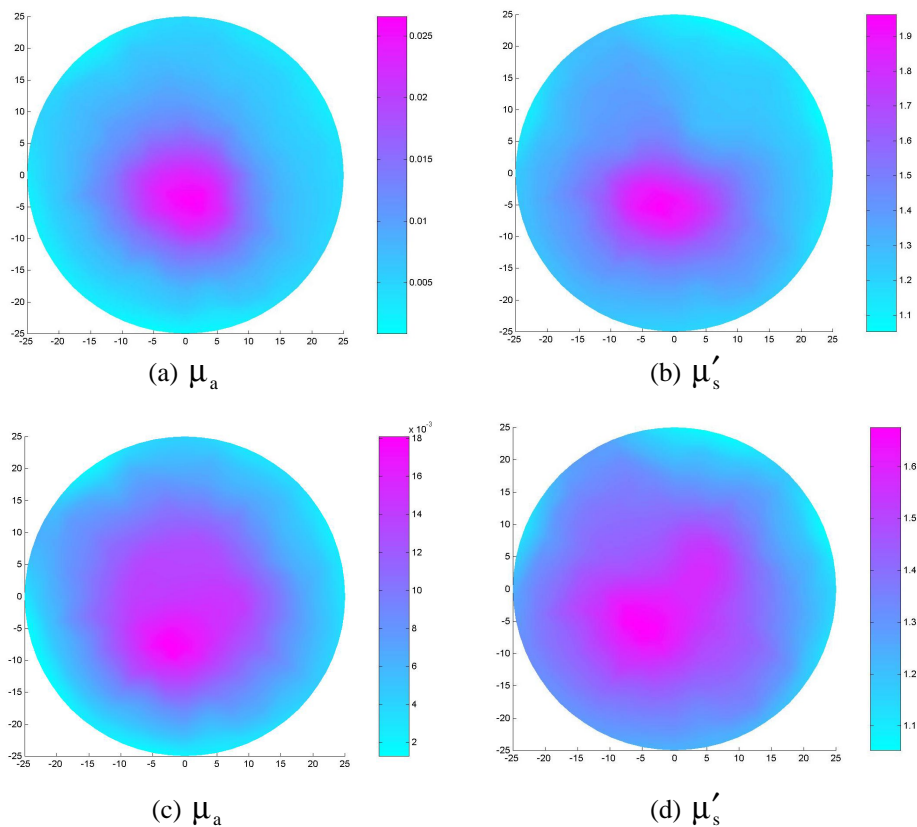


Fig. 3: Reconstructed μ_a (mm^{-1} , absorption) and μ'_s (mm^{-1} , reduced scattering) images from phantom/bones measurements. (a) and (b): images at measurement plane 1. (c) and (d): images at measurement plane 2.

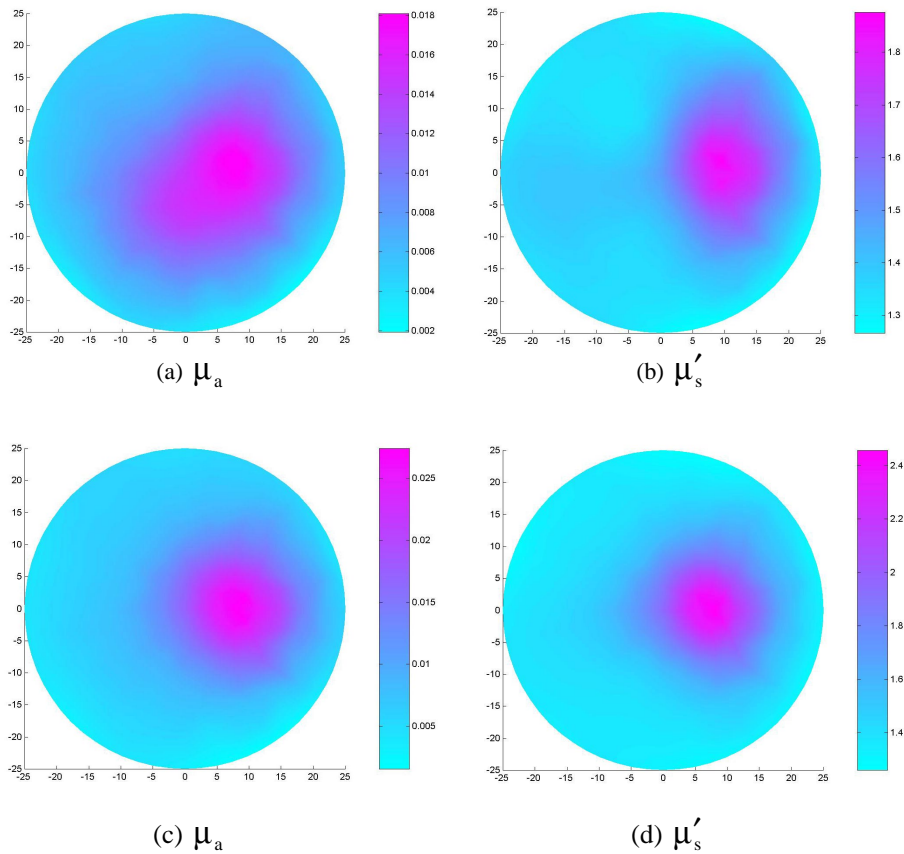


Fig. 4: Reconstructed μ_a (mm^{-1} , absorption) and μ'_s (mm^{-1} , reduced scattering) images from the in vivo measurements obtained around the proximal interphalangeal (PIP) joint of the index finger (the pinkish region corresponds to the finger; the bluish background corresponds to the solid phantom). (a) and (b): images at the joint plane. (c) and (d): images at the off-joint/bone plane.

In summary, we have demonstrated in vivo and in vitro that bone and joint tissues can be quantitatively imaged by DOT. Since normal and diseased joint/bone tissues show clear differences in both absorption and scattering coefficients,^{11,12} this work suggests that DOT may become a useful tool for detecting and monitoring joint/bone diseases such as osteoporosis and arthritis.

Acknowledgements

This research was supported in part by grants from the National Institutes of Health (NIH) (AR 46427), and the Department of Defense (DOD) (BC 980050).